Title: Cr-free Cu-catalysts for the selective hydrogenation of biomass-derived furfural to 2-methylfuran: The synergistic effect of metal and acid sites

Author: Fang Dong Yulei Zhu Hongyan Zheng Yifeng Zhu Xianqing Li Yongwang Li

PII: S1381-1169(14)00539-1
DOI: http://dx.doi.org/doi:10.1016/j.molcata.2014.12.001
Reference: MOLCAA 9363

To appear in: *Journal of Molecular Catalysis A: Chemical*

Received date: 11-10-2014
Revised date: 20-11-2014
Accepted date: 3-12-2014

Please cite this article as: Fang Dong, Yulei Zhu, Hongyan Zheng, Yifeng Zhu, Xianqing Li, Yongwang Li, Cr-free Cu-catalysts for the selective hydrogenation of biomass-derived furfural to 2-methylfuran: The synergistic effect of metal and acid sites, Journal of Molecular Catalysis A: Chemical http://dx.doi.org/10.1016/j.molcata.2014.12.001

Cr-free Cu-catalysts for the selective hydrogenation of biomass-derived furfural to 2-methylfuran: the synergistic effect of metal and acid sites

Fang Dong [a,b,c], Yulei Zhu [a,c,*], Hongyan Zheng [c], Yifeng Zhu [a,b], Xianqing Li[c], Yongwang Li [a,c]

[a] *State Key Laboratory of Coal Conversion, Institute of Coal Chemistry, Chinese Academy of Sciences, Taiyuan 030001, PR China*

[b] *Graduate University of Chinese Academy of Sciences, Beijing 100039, PR China*

[c] *Synfuels China Co. Ltd., Taiyuan 030032, PR China*

[*]Corresponding author: *State Key Laboratory of Coal Conversion, Institute of Coal Chemistry, Chinese Academy of Sciences, Taiyuan 030001, PR China.* Tel.: +86 351 7117097; fax: +86 351 7560668.

E-mail address: zhuyulei@sxicc.ac.cn (Y. Zhu).

Abstract

Our work focuses on exploring Cr-free Cu-catalysts for the highly efficient conversion of biomass-derived furfural to value-added bio-fuel 2-methylfuran. Three supported Cu-catalysts (Cu/SiO_2, Cu/Al_2O_3, and Cu/ZnO) were prepared by the typical precipitation method, and Cu/SiO_2 catalyst exhibited the best catalytic performance with an 89.5 % yield to 2-MF. A series of characteristic results indicated that the high yield of 2-methylfuran on Cu/SiO_2 catalyst was assigned to synergistic effect of metal and the weak acid sites. Among them, Cu/ZnO catalyst exhibited maximum furfuryl alcohol selectivity because of the large Cu particles, while Cu/Al_2O_3 catalyst had low 2-methylfuran selectivity due to the insufficient weak acid sites. For Cu/SiO_2 catalyst, the highly dispersed Cu particles and the strong metal-support interaction are propitious to its superior catalytic activity. Therefore, copper species are composed on different supports as a result of the different interaction of metal-support to affect their catalytic activity, while products selectivity is related to the acidic property of catalyst. In addition, temperature programmed desorption of furfural indicated that the adsorption-desorption properties of catalyst surface species would influence the rate of furfural hydrogenation.

Keywords: furfural; *catalytic hydrogenation; 2-methylfuran; Cu-catalysts; support effects*

1. Introduction

With the fossil resources reducing, the development and use of biomass resource, as well as biomass derives has been more and more pressing [1-4]. And Grilc et. al [5,6] have also reported that petroleum refining-based catalysts employing mono-(Ni, Co and Mo) and bi-functional catalysts have been proved as being rather efficient and cost effective for hydrogenation and deoxygenation of biomass and biomass-derived compounds. Furfural (FAL) is treated as one of the important platform molecules in biomass conversion, and its source is very wide, inexpensive, and environmental. FAL is massively produced from carbohydrate biomass obtained from agricultural wastes such as corncobs, wheat-straw, and bagasse, which carry through the catalytic dehydration process [7]. FAL could be converted into all kinds of containing-oxide chemicals such as furfuryl alcohol (FOL), 2-methylfuran (2-MF), 2-methyltetrahydrofuran, and tetrahydrofurfuryl alcohol [8-10]. Among these chemicals, value-added bio-fuel 2-MF by hydrogenation-deoxygenation process of FAL generated a great interest because of good fuel performance of 2-MF [11]. Unlike hydrocarbons, 2-MF contains the oxygen atom with the better combustion performance and the higher energy density. Especially, research octane number (RON=103) of 2-MF is higher than that of gasoline (RON=96.8), and it would be regarding as gasoline alternative to increase the performance on anti-explosion [12,13]. Conventional process for the production of 2-MF relies on the petroleum resources and requires the catalytic oxidation, an example being the oxidation of 1,3-pentadiene from the fossil energy. From the viewpoint of green sustainable chemistry, the production of 2-MF from biomass-derived chemicals is highly desirable. Therefore, the conversion of FAL to 2-MF could not only relieve the fossil energy crisis, but utilize effectively a large number of surplus biomass resources. However, it is a challenging job for catalytic researchers to develop an environmentally friendly catalyst for the highly efficient conversion of FAL to 2-MF.

Cu-based catalysts have been reported as the most promising candidate for the conversion of FAL to 2-MF [14]. Industrial production of 2-MF is performed on Cu-Cr catalysts for decades. However, the heavy environmental pollution and energy crisis limited the wide use of Cu-Cr catalysts, and the high toxicity has enforced the researchers to develop the high active Cr-free catalysts [15-17]. Moreover, the sustainability of this platform also requires the invention of novel and efficient catalysts for achieving the high yield of 2-MF, so the development of catalysts is very significant. Although many studies that have been reported employed Cu/MgO [18], Cu/C [19], and Ni-Fe [20] as catalysts in FAL hydrogenation reaction, the yield of 2-MF was still low. Yan et

al. [21] also studied the Cu-Cr catalyst for the hydrogenation of FAL and levulinic acid to FOL and ɤ-valerolactone, respectively. R. Rao et al. [22] reported that the Cu^{+} and Cu^{0} sites of Cu-Cr catalyst surface were responsible for the maximum activity in the catalytic process, which produced as a function of reduction temperature. In addition, some common hydrogenation-deoxygenation catalysts include precious metal, such as Ru [23], Rh [24], Pd [25], and Re [26], which have low selectivity due to some undesirable side reactions involving C-C bond cleavage and the high cost of catalysts. Therefore, most of catalysts are unsuitable for the industrial application owing to some defects, such as serious environmental pollution, the low selectivity, the high cost, and severe deactivation.

Our previous works [27] have suggested a reaction pathway carried out **scheme.1** for the formation of FAL hydrogenation on Cu-catalysts. It is well-known that hydrogenation of FAL to 2-MF included hydrogenation of FAL to FOL, and followed by subsequent hydrogenolysis-deoxygenation of the intermediate FOL to desired product 2-MF. Most of previous studies reported that the Cu active sites are answering for the selective hydrogenation of C=O bond, and relatively inactive for hydrogenolysis of the saturated C-O bond [28,29]. Lewis acid sites would be beneficial to the breaking of the saturated C-O band [20,30]. Thus, the appropriate combination of metal components and acidic species in reaction system is indispensable for the effective formation of 2-MF. Notably, the nature of supports might influence the surface acidity and basicity of catalysts which plays the vital roles in products distribution. However, little work has been done to report about support effects on the texture and chemical characteristics of copper catalysts, as well as their catalytic performance in FAL hydrogenation reaction. Therefore, some Cr-free, environmental, and low cost supports, such as SiO_2, Al_2O_3, and ZnO (easy to be applied in industry), are chosen in our work.

The purpose of this work is to investigate some environmentally friendly Cr-free Cu-catalysts supported on SiO_2, Al_2O_3 and ZnO surface, with the help of systematical characterizations, to explain the roles of support on copper dispersion, the interaction of metal-support, surface acidity and FAL hydrogenation activity. For SiO_2 support, a strong interaction of copper-silicon might result in a higher copper dispersion, the difficult reduction of copper oxide, and the stronger acidic property than the other two samples to improve the catalytic performance. In the case of Al_2O_3 and ZnO supports, a weak interaction favors the reducibility of copper oxide, but at the same time

promotes the agglomeration of copper particles leading to a low copper dispersion. Therefore, Cr-free Cu/SiO_2 catalyst would be treated as a promising candidate applied to the production of 2-MF.

2. Experimental

2.1. Catalyst preparation

Three different catalysts (Cu/SiO_2, Cu/Al_2O_3, Cu/ZnO) were prepared by the precipitation method. In a typical preparation process, the aqueous solutions of $Cu(NO_3)_2.3H_2O$ mixed respectively with silica sol (SW-30), Alumina sol (AS-40), and $Zn(NO_3)_2.6H_2O$ solution. Then three mixed aqueous solution and 1M NH_4HCO_3 solution were simultaneously added drop wise to 200 mL deionized water under the vigorous stir, and pH value was kept in the range of 6.0-7.0. The obtained slurry was further aged for 1.0 h, and then the suspension was washed and filtered. Subsequently, the precipitate was dried at 120 ºC for 24 h in air. After this, the obtained precursors were calcined under 450 ºC for 5 h with a heating rate of 1 ºC/min in air. Finally, the Cu/M_xO_y (M=Si, Al, Zn) precursors were obtained. The reference sample of CuO was prepared by the same method similar to that reported previously [31].

2.2. Catalyst characterization

N_2 adsorption-desorption isotherms of calcined catalysts were obtained at -196 ºC using an ASAP 2420 (Micromeritics, Inc). Prior to N_2 adsorption, all samples were degassed under vacuum at 90°C for 1 h and 350°C for 8 h. After degassed, BET surface area and BJH pore size distribution were calculated according to the desorption branch of the isotherms.

ICP optical emission spectroscopy was performed on Optima2100DV, PerkinEl-mer.

X-ray diffraction (XRD) patterns were collected on a BrukerAxs D8 diffractometer with Cu Kα radiation (λ=0.154 nm) at 30 kV and 10 mA with a scanning angle (2θ) ranging from 10º to 80º at the scanning rate of 4º/min to determine the crystalline phases.

The microstructural observations and analysis of catalyst surface were performed using a scanning electron microscope (SEM, FEI Quanta 400F) and an energy dispersive X-ray spectrometer (EDS). Before the EDS test, the grinded catalyst was pressed into a tablet.

The reducibility of the calcined samples was determined by H_2-temperature programmed reduction (H_2-TPR), which performed on Auto Chem. II2920 (Mircromeritics, USA). Before reduction, 200 mg samples were put into a quartz tube, then it was carried out using a heating rate of 5 °C /min from 40 °C to 500 °C in a 10 vol% H_2/He mixture at a flow rate of 50 $cm^3.min^{-1}$, and

the single was recorded with TCD apparatus. A 2-propanol-liquid nitrogen slurry (−89 °C) cooled trap was used to cool the water formed during the reduced process.

N_2O measurements were conducted in the same equipment as H_2-TPR using 200 mg samples for each test. Before analysis, the CuO phase is completely reduced to metal copper with a flow mixture of 10 vol% H_2/He. Then, the catalyst is purged under He. Orderly, the oxidation of surface metal copper to Cu_2O is carried out by chemisorption of N_2O (5 vol% N_2O/He) at 90 ºC. After that, the catalyst was purged with a He flow gas and cooled to room temperature. Subsequently, H_2-TPR was again carried out (similar to the former reduction process), in order to reduce the surface Cu_2O to metal copper. Copper dispersion (D_{Cu}) was calculated by dividing the amount of chemisorption sites into total supported copper atoms; the copper surface area (S_{Cu}) was calculated by assuming spherical shape of the copper metal particles and 1.47×10^{19} copper atoms/m^2.

X-ray photoelectron spectroscopy (XPS) studies were performed with a Physical Electronics PHI 5700 spectrometer equipped with a Mg Kα (1253.6 eV) X-ray source. Before XPS analysis, 200 mg samples were reduced in pure H_2 at 270 °C, using a flow rate of 50 mL/min about 2 h.

Temperature programmed desorption of NH_3 (NH_3-TPD) was performed on the same instrument as H_2-TPR. Prior to the adsorption of NH_3, 200 mg samples were pretreated with He gas at 400 ºC to clean surface impurities from moisture and other adsorbed gases. After cooling to 100 ºC, the catalyst was saturated with pure NH_3 and then purged with He gas to remove the physisorbed NH_3. Subsequently, the sample was heated to 800 ºC at a heating rate of 10 ºC/min and the NH_3 desorption (m/z=16) was detected by MS (Agilent).

Temperature programmed desorption of H_2 (H_2-TPD) over three supported Cu-catalysts was performed on the same instrument with H_2-TPR. Prior to H_2 absorption, 200 mg samples were put into the quartz tube reactor, and reduced in pure H_2 (50 mL/min) gas flow at 270 ºC for 2 h. Subsequently, the sample was purged at 270 ºC with He (50 mL/min), then the sample was cooled to 30 ºC with He gas flow. After this, the sample was heated to 800 ºC at 10 ºC/min with a He gas, and the H_2 desorption (m/z=2) was detected by a MS (Agilent).

Temperature programmed desorption of furfural (FAL-TPD) was performed in a self-made reactor connected to an online mass spectrometer (OmniStar TM). Before desorption 200 mg calcined catalysts were reduced by pure H_2 at 270 °C for 2 h, and then purged with He at the same temperature and cooled to 40 °C overnight in order to diminish the effect of H_2. Thereafter, reduced catalysts were performed in FAL/He flow at 40 ◦C for 2 h, in order to absorb sufficient furfural. After the absorption, samples were purged with He for removing the physical adsorbed

FAL at 40 °C until the baseline was stable. Finally, the FAL-TPD experiment was performed with a heating rate of 10 °C/min in a flow of He stream from 40 °C to 800 ºC, and the desorbing products were detected with an online MS (Agilent).

2.3. Catalytic test and analysis method

FAL hydrogenation was carried out in a fixed-bed reactor (12 mm of inner diameter, length of 600 mm). First of all, all the samples were completely reduced in situ at atmospheric pressure with a 5 vol. % H_2/N_2 gas mixture at 270 °C. After reduction, the distilled FAL was continuously pumped to a preheater by HPLC pump, and the preheater was maintained at 140 °C to prevent condensation of vaporized FAL. At the same time, H_2 was introduced into the top of preheater through mass flow controller. Thereafter, FAL vaporizer mixed with pure hydrogen in the preheater and then introduced into the fixed-bed reactor. Typical reaction conditions for FAL conversion were as follows: 140-220°C, atmospheric pressure and weight hourly space velocity (WHSV) = 0.5, 2.0 h^{-1}. The reaction products were condensed and collected in a gas-liquid separator, which were analyzed by the chromatography until all conditions of the reaction system was stable. The liquid products were analyzed by an off-line gas-chromatography (GC6890, Agilent, USA) using a FID detector and polyethandiol capillary column (AB-inowax, 30 m×0.32 mm), and the gas products were analyzed by an on-line GC 6890 (Aligent, USA) equipped with a FID detector and polyethandiol capillary column (AB-inowax, 30 m×0.32 mm). **P**art of products need to be identified by a GC-MS (6890N, Agilent, USA). The carbon balance was typically better than 96% and the error associated with the quantification for furfural was found to be about ±3%. The conversion, selectivity and carbon balance were calculated on basis of the following equations:

$$\text{Conversion}(\%) = \frac{\text{Mole of furfural converted (mol)}}{\text{Mole of furfural fed (mol)}} \times 100$$

$$\text{Selectivity}\,(\%) = \frac{\text{Mole of the product produced (mol)}}{\text{Mole of furfural converted (mol)}} \times 100$$

$$\text{Carbon balance}(\%) = \frac{\text{Mole of the overallcarbon fed (mol)}}{\text{Mole of the overall carbon outflowed (mol)}} \times 100$$

TOF was calculated to investigate the intrinsic catalytic activity, which was defined as the number of molecules of a specified product made per catalytic site and per unit time. In this paper TOF was calculated in a low activity.

3. Results and discussion

3.1. Textural Properties of the Catalysts

The physicochemical properties of the calcined catalysts are presented in **Table 1**, and an obvious distinction of BET surface area (S_{BET}) was observed over three supported Cu-catalysts. Especially, Cu/SiO_2 catalyst exhibited the largest BET surface area (161.4 $m^2.g^{-1}$). The decline of BET surface area (from 161.4 to 14.9 $m^2.g^{-1}$) and pore volume (from 0.430 to 0.134 $cm^3.g^{-1}$) might be attributed to the nature of support substrates [32]. Copper dispersion (D_{Cu}) is the vital parameter, which greatly influences the physicochemical properties and the catalytic performance of catalyst [33]. As shown in **Table 1**, copper dispersion from N_2O chemisorption (Table 1) followed the sequence of Cu/SiO_2 > Cu/Al_2O_3 > Cu/ZnO. In addition, N_2 adsorption-desorption isotherms are shown in **Fig. 1S**. Cu/SiO_2 and Cu/Al_2O_3 samples exhibited isotherms with the typical hysteresis loops of mesoporous materials. Adsorption for Cu/ZnO sample shifted toward higher values, indicating the presence of larger pores.

The XRD patterns of three Cu-catalysts obtained after calcination at 450 ºC are shown in **Fig. 1**. The peaks at around 35.5ºand 38.9º (JCPDS 05-0661) are attributed to the collective contribution of crystalline CuO, and the distinction of XRD patterns on these supported Cu-catalysts may be linked to the existence of different copper species and the size of copper crystalline [29]. Based on the Scherrer equation, the copper crystallite size of three supported Cu-catalysts was respectively 8.5, 11.4 and 14.5 nm according to the full width at half maximum of Cu (111) diffraction at 2θ of 38.7º. Evidently, Cu/SiO_2 catalyst showed the smallest crystalline size.

The SEM and face scanning energy dispersive spectrum (face scanning EDS) images of three supported Cu-catalysts are exhibited in **Fig. 2S**. The purpose of energy dispersive X-ray spectrometry (EDS) investigation is to characterize the homogeneity and determine the copper concentration of catalyst surface. The contents of element are listed in **Table 1S**. Based on the results of face scanning EDS, there were some aggregated and highly dispersed fields, suggesting the existence of big copper particles and small copper particles. Overall, copper particle was more uniform on Cu/SiO_2 catalyst than the other two samples. The total copper contents, as determined by EDS, are consistent with ICP-AES in **Table 1**.

3.2 Reduction properties and Chemical states of catalysts

3.2.1 Reduction properties of catalysts

H_2-TPR was used to determine the reducibility of these supported Cu-catalysts, and **Fig. 2** displays H_2-TPR profiles of the calcined samples. Generally, when copper species interacted with supports by forming new surface compounds or changing the chemical states of copper, their

reduction temperature would change [33,34]. Therefore, the interactions of copper components with supports had significant influence on the chemical environment of copper, and a weak interaction would be easy to reduce copper oxide to metal copper [35]. On the contrary, when a strong interaction between copper species and supports occurred, CuO particles would be difficultly reduced, and this reduced process might turn up low valence copper such as uncompleted reduced Cu^{+}. The difference of H_2-TPR cannot be solely explained in terms of copper dispersion, also including the CuO crystallinity size and the interaction of copper-support [32]. Among three factors mentioned in front, the interaction between metal and support may play a key role in determining the reduction temperature in our system. Firstly, the reduction temperature of three samples was higher than that of pure CuO (**Fig. 2**). In addition, the asymmetric reduction peak of samples indicated that there were at least two different Cu species, which might be attributed to two closely overlapping peaks of dissimilar intensities [33], reflecting reduction in two steps ($Cu^{2+} \rightarrow Cu^{+}$ at low temperature, $Cu^{+} \rightarrow Cu^{0}$ at high temperature). The difference of the reduction temperature illustrated that SiO_2 (228 ºC) support had the stronger interaction with copper species than Al_2O_3 (217 ºC) and ZnO (202 ºC) supports. Obviously, the variation of H_2-TPR peak sites states the strength of interaction, indicating that supports have great influence on the reduction of copper oxide.

For three supported Cu-catalysts, the interaction is strongest when copper oxide was dispersed on SiO_2 support. The reduction process ($Cu^{2+} \rightarrow Cu^{0}$) occurred more difficult and slower, and resulted in the smaller copper oxide particles or the better copper oxide dispersion on SiO_2 support surface. The result of H_2-TPR is in agreement with XRD result.

3.2.2 The surface chemical states of catalysts

The chemical states of copper species were determined by XPS analysis, and the spectrum of both the calcined catalysts and the reduced catalysts is recorded in **Fig. 3**. The calcined samples (**Fig. 3A)** displayed the main peak (Cu $2p_{3/2}$) above 933.8 ± 0.2 eV, which was attributed to the copper oxidation state as +2 [36]. Similarly, the spectrum of the reduced samples showed a significant shift of the main peak (Cu $2p_{3/2}$) towards the lower binding energies at 932.6 eV, which were because of the reduction of surface Cu^{2+} to the lower valence states [37] (**Fig. 3B)**. Meanwhile, the absence of satellite peaks at 944-945 eV (2p-3d) related to Cu^{2+} were observed at all of the reduced samples, suggesting that the Cu^{2+} species (mainly from copper oxide) were reduced completely. The reduced samples are probably inferred to have two species Cu^{+} and Cu^{0} at 932.6 eV, which is impossible to make a distinction between Cu^{+} and Cu^{0} on the basis of binding energy analysis alone. Following, we carried out the examination of the modified Auger spectra (XAES). The broad and asymmetric peak shape of the Cu LMM XAES spectra (**Fig. 3C**)

indicated that the reduced samples could have one more chemical states of copper. The asymmetric peaks were fitted with two symmetrical peaks: α and β, which centered at around 916.1 eV and 919.2 eV, corresponding to Cu^{+} and Cu^{0}, respectively. According to the data fitting results, Cu/SiO_2 catalyst had the higher Cu^{+}/Cu^{0} than the other two samples (**Table 1**). Copper oxide on the sample surface could not be reduced totally to metal copper, and these Cu^{+} species might be generated from Cu^{2+} species interacting with support after reduction [32]**.** In previous works, the raise of hydrogenolysis activity for the supported metal catalysts had been attributed to electron-deficient of the active metal and support [38,39]. The deficient of the active metal can result from the donation of metal electron density to support. In our studies, the more Cu^{+} species of Cu/SiO_2 catalyst might be attributed to the higher electron affinity of silicon. It is suggested that SiO_2 support has an important influence on the electronic structure of the active copper, which is accordance with CO-FTIR analysis results (**Fig. 3S**).

3.3 The surface acidic properties of the catalysts

In order to explore surface acidity, NH_3-TPD was performed on three supported Cu-catalysts (**Fig. 4**). Generally, the strength of acid sites which is determined by the NH_3 desorption temperature is classified as three types, weak acid (150–300 ºC), medium acid (300–500 ºC), and strong acid (500–650 ºC) [40]. In our work (**Fig. 4A**), Cu/Al_2O_3 sample showed a main peak at 170 °C, which could be attributed to NH_3 desorption from the weak acid sites. Besides, there was a minor peak at 400°C related to the medium acid of Cu/Al_2O_3 surface as a result of the nature of support. For Cu/ZnO sample, an obvious peak at 330°C might be assigned to NH_3 desorption from the medium acid sites produced probably by an extremely weak interaction of metal-support, and accompanied with a faint peak at 170 °C. Evidently, Cu/SiO_2 catalyst showed the largest peak at around 190 ºC, indicating that it has much more the weak acid sites than the other two samples. In addition, we also verified that pure CuO and SiO_2 had scarcely the acidic property, but the reduced Cu/SiO_2 catalysts produced a huge amount of the weak acid sites (**Fig. 4B**). These new weak acidic sites may be related to some low state copper species, such as Cu^{+} [39,41,42], which result from the strong interaction of copper- silicon. Some copper species may still interact with SiO_2 support after reduction, and the deficient of these copper species may be derived from the high electron affinity of silicon. This affinity of silicon would seize electrons from metal copper. The transfer of electron density from metal copper to silicon would increase the electropositive (or the oxophilic nature) of copper, and in further the improving of the oxophilic nature would contribute to hydrogenolysis of the saturated C-O band. Therefore, acid quantity and types of Cu-catalysts, especially the acid types, can be modulated by using some different acid/basic supports to produce the new active sites

3.4 Temperature programmed adsorption-desorption experiments

Fig. 5 shows the ability of desorption hydrogen, which absorbed surface and subsurface of these supported Cu-catalysts. The obvious desorption peak of hydrogen occurred for all of samples at near 58 ºC, and this desorption peak might be assigned to the desorption of hydrogen from copper surface [43,44]. A minor desorption peak was exhibited to Cu/Al_2O_3 sample about 200 ºC, and this was probably linked to the function of Al_2O_3 support [45]. Besides, Cu/ZnO sample about 350°C came up a broad peak, which might be related to the hydrogen desorption from ZnO support or the interface of copper particles with support. It is known that ZnO is capable of occluding large amounts of hydrogen both on the surface and in subsurface regions [46]. For Cu/SiO_2 catalyst, the desorption peak of hydrogen came up at 58 ºC with the highest desorption amount, and presented hardly the desorption peak at high temperature.

FAL-TPD experiments were done to explore the stability and strength of surface species during desorption process over three supported Cu-catalysts in range of 40-800 ºC. Mass characteristics of different desorption products are shown in **Fig. 6**, including FAL ($C_5H_4O_2$, m/e = 96), FOL ($C_5H_6O_2$, m/e = 98), 2-MF (C_5H_6O, m/e = 82), and H_2O (m/e = 18).

Fig. 6A (FAL, m/e=96) displays the desorption of reactant FAL. Desorption amount of FAL is highest on Cu/SiO_2 catalyst, and the desorption temperature of FAL followed the sequence of Cu/SiO_2 > Cu/Al_2O_3 > Cu/ZnO. First, Cu/SiO_2 catalyst had the higher copper dispersion and BET surface area than the other two samples, hence adsorption amount of FAL is sufficient. On the other hand, the desorption temperature of FAL is higher than the other two samples. The two reasons may enhance the concentration of reactant FAL on Cu/SiO_2 surface, and in further would increase the rate of FAL hydrogenation process.

According to **Fig. 6B** (FOL, m/e=98), the desorption of FOL from products of FAL hydrogenation is similar to FAL desorption on three supported Cu-catalysts. It is also found that desorption temperature of FOL on Cu/SiO_2 catalyst is higher than the other two samples, that is to say, FOL is also hard to desorb from Cu/SiO_2 surface. Successively, the rate of FOL hydrogenolysis reaction may be increased with increasing the concentration of the intermediate FOL on the catalyst surface.

Likely, **Fig. 6C** (2-MF, m/e=82) shows the desorption of desired product 2-MF from hydrogenolysis of the intermediate FOL. Desorption amount of 2-MF followed the sequence of Cu/SiO_2 > Cu/Al_2O_3 > Cu/ZnO, and the desorption temperature of 2-MF on Cu/SiO_2 catalyst is lowest among three catalysts. Notably, the rate of hydrogenolysis reaction would increase with decreasing the concentration of product 2-MF on catalyst surface. The largest desorption amount

of 2-MF on Cu/SiO_2 catalyst might be assigned to the sufficient weak acid sites and the highest Cu^+/Cu^0 value, which could offer the more sufficient active sites to convert the intermediate FOL to desired product 2-MF than the other two samples.

Fig. 6D (H_2O, m/e=18) expresses the desorption of water, which come mainly from the hydrogenolysis of the intermediate FOL. When the intermediate FOL is converted into 2-MF, this process would produce the equimolar amount of water. It is found that the desorption temperature of H_2O on Cu/SiO_2 catalyst is the lowest among three catalysts, which is consistent with the desorption of 2-MF.

Overall, Cu/SiO_2 catalyst had the sufficient adsorption amount of reactant FAL and the fast desorption rate of desired product 2-MF. Adsorption of reactant FAL, conversion of the intermediate FOL, and desorption of desired product 2-MF would have effects on the yield of product 2-MF on Cu-catalysts surface, suggesting that the adsorption-desorption properties of surface species would influence the rate of furfural hydrogenation

3.5 Catalytic performance in FAL hydrogenation

3.5.1. The effect of supports for the activity and the selectivity

In order to investigate support effects on catalytic performance of Cu-catalysts, we tested the activity of all of samples (**Table 2 and Fig. 4S**). Obviously, hydrogenation activity of Cu/SiO_2 sample was much higher than the other two samples, and showed the highest yield of 2-MF. FAL conversion and selectivity of 2-MF were as high as 100 % and 89.5 %, respectively. For Cu/ZnO sample, FAL conversion and selectivity of 2-MF were both lowest among three samples. FAL conversion on Cu/Al_2O_3 catalyst is next only to Cu/SiO_2, but 2-MF selectivity of Cu/Al_2O_3 catalyst is a lot lower than that of Cu/SiO_2. The former literature reported that the vapor-phase hydrogenation of FAL was performed on $Ni\text{-}Fe/SiO_2$ catalyst resulted in a 39.1 % selectivity to 2-MF [20]**.** The vapor-phase hydrogenation of FAL carried out at 250 °C in a fixed bed reactor over a multicomponent commercial catalyst (Cu: Zn: Al: Ca: Na=59:33:6:1:1) afforded an 87 % selectivity to 2-MF [27]. The hydrogenation of FAL in supercritical CO_2 ran up to a 90 % selectivity of 2-MF over Cu-Cr catalyst at 240 °C [47]. Notably, we used Cr-free Cu/SiO_2 catalyst for the vapor-phase hydrogenation of FAL, selectivity of 2-MF was as high as 89.5 % and FAL was completely converted at 220 °C, 1 atm. The compared results (**Table 3**) suggested that Cu/SiO_2 catalyst could convert FAL into 2-MF at a lower temperature, and gain the good yield of desire product 2-MF. In combination with FAL-TPD (**Fig. 6**) experiments, the more adsorption amount of FAL was found on Cu-catalysts surface, the higher conversion of FAL was discovered. On the other hand, the lower desorption temperature of 2-MF were discovered on Cu-catalysts surface, the higher selectivity of 2-MF also brought. In addition, the desorption rate of 2-MF was

fastest on Cu/SiO_2 catalyst, and it was properly explained that the rate of FAL hydrogenation increased with increasing the concentration of reactant (FAL), meanwhile, the reaction rate increased with the decrease of the desorption temperature and the concentration of product on catalyst surface. FAL-TPD experiments are in very good agreement with the obtained experimental data displayed in **Table 2**.

Turnover frequency (TOF) is calculated to explore the intrinsic activity of these supported Cu-catalysts [48]. The results (**Table 2**) suggested that Cu/SiO_2 catalyst achieved the highest TOF, up to 24.3 h^{-1}, which is obviously superior to the other two samples. Among these Cu-catalysts, FAL conversion and selectivity of 2-MF are found to be in the order: Cu/SiO_2 > Cu/Al_2O_3 > Cu/ZnO. The test results clearly confirmed that Cu/SiO_2 catalyst showed the best catalytic activity for FAL hydrogenation. Because SiO_2 support could interact with copper species to disperse uniformly copper particles with the higher loading of Cu^0 and Cu^+, which might be important for catalytic reaction such as FAL hydrogenation exemplified here, and active sites was sufficient to convert FAL into other products. Among these Cu-catalysts, Cu/ZnO exhibited maximum furfuryl alcohol selectivity because of the large Cu particles, while Cu/Al_2O_3 catalyst had low 2-MF selectivity due to the insufficient weak acid sites. Moreover, it is probably concluded the adequate weak acid sites on Cu/SiO_2 surface made the intermediate FOL convert into 2-MF by the hydrogenolysis process. These weak acid sites which had the strong oxophilic nature for the saturated C-O band might promote C-O band hydrogenolysis, which is also in accordance with Sitthisa's work [20,49]. Hydrogenation of FAL to FOL might be catalyzed by the active sites of Cu even at low temperature (140 ºC), and hydrogenolysis of the intermediate FOL is motivated by the oxophilic nature of metal acid sites, which were probably attributed to Lewis acid sites (Cu^+). Moreover, XAES results also suggested that Cu/SiO_2 catalyst had a higher Cu^+/Cu^0 than the other two samples, which might function as electrophilic or Lewis acid sites to polarize the saturated $-CH_2$-OH band via the electron lone pair on oxygen [50].

3.5.2. Influence of the reaction conditions over Cu/SiO_2 catalyst

Among three supported Cu-catalysts, Cu/SiO_2 catalyst exhibited a promising catalytic performance, since the following investigations of the reaction temperature and weight hourly space velocity (WHSV) were conducted on this sample.

(1) Influence of the reaction temperature

Influence of the reaction temperature on Cu/SiO_2 is shown in **Table 4**. Evidently, FOL is the main product at low temperature (140 ℃), and selectivity of 2-MF is sharply increased with increasing the reaction temperature from 140 to 220 ºC. As expected, FAL conversion increased from 98.3 % (140 ℃) to 100 % (200 ℃) and then remained at 100 % as the temperature elevated

(WHSV=0.5h^{-1}). Selectivity of 2-MF increased remarkably with increasing temperature, and as high as 89.5 % at 220 °C, WHSV=0.5h^{-1}. Simultaneously, selectivity of pentanone and pentanol also increased with increasing temperature. It is apparently seen that selectivity of 2-MF at lower temperature (<180 °C) was very low, due to the existence of the intermediate FOL, whereas the decrease of selectivity at higher temperature was related to the formation of undesired by-products, such as the overhydrogenolysis products 2-pentanone, 1-pentanol, and 2-pentanol, indicating that the reaction temperature is an important condition to enhance selectivity of 2-MF, which is in accordance with our former work [27,51].

(2) Influence of Weight hourly space velocity

Influence of weight hourly space velocity (WHSV=0.5 h^{-1} and 2.0 h^{-1}) for the FAL hydrogenation reaction over Cu/SiO_2 was studied, and the results are showed in **Table 4**. Conversion of FAL dropped obviously with increasing WHSV at lower reaction temperature (<180 ºC), while the conversion of FAL was a little decline with increasing WHSV at higher temperature (>200 ºC). Concurrently, WHSV, high and low, FOL was the main product at low temperature (<160 ºC), but selectivity of 2-MF increased rapidly with decreasing WHSV above 160 ºC. When the reaction temperature increased to 220 °C, influence of WHSV was inconspicuous. Therefore, the raise of temperature is much more prominent for the $-CH_2-OH$ hydrogenolysis of the intermediate FOL than the falling of WHSV on Cu/SiO_2 catalyst. In addition, FOL was the main product at high WHSV, because the residence time shortened correspondingly, and FOL had no time to convert in a step further, suggesting that the long residence time favors the acceleration of sequential hydrogenolysis of the intermediate FOL to 2-MF.

3.5.3. The stability of Cu/SiO_2 catalyst

Since Cu/SiO_2 catalyst presented the best 2-MF selectivity, the long term stability of this sample was also explored. As illustrated in Fig. 7, the Cu/SiO_2 catalyst did not present any distinct loss in the activity within 210 h time-on-stream under high temperature (220 °C). Concurrently, 2-MF selectivity did not show obvious fluctuation during the complete test, indicating that the Cu/SiO_2 catalyst was robust under the test conditions. TEM images of the fresh and spent samples provided clues concerning the good stability of Cu/SiO_2 catalyst. As displayed in Fig. 8, similar the TEM images (Fig. 8) of the fresh and spent catalysts demonstrated the Cu particles were not obviously sintered after the long term reaction (210 h). In total, the superior stability of Cu/SiO_2 catalyst lies in the strong interaction of the active components with support SiO_2, which was responsible for the stable structure of catalyst and improved the catalytic properties.

The evolution of catalytic activity on three supported Cu-catalysts states clearly synergistic

effect of copper dispersion and the acidic property for the selective hydrogenation of FAL to 2-MF, which is favorable to activate the -CH=O group of reactant FAL and cleave the saturated -CH_2-OH group of the intermediate FOL. Among three supported Cu-catalysts, when copper ions were dispersed on SiO_2 support, the interaction was the strongest. This strong interaction would not only elevate copper dispersion, but also be favorable to enhance the Cu^+ sites of catalyst surface and the weak acid amount. The literature [22] reported that that the maximum activity of Cu-Cr catalyst was attributed to the co-existence of Cu^+ and Cu^0 sites on the catalyst surface. Concurrently, the long term stability of Cu/SiO_2 catalyst was exhibited about 210 h without an obvious loss in the activity of catalyst and the major products selectivity, and the good stability might be due to the strong interaction of copper-silicon. In next work, it is important in further to explore the mechanism of FAL hydrogenation on Cu/SiO_2 catalyst and develop a better copper-silicon catalyst which could be applied to the industrial production.

4. Conclusions

Three supported Cu-catalysts were tested for the selective hydrogenation of FAL to bio-fuel 2-MF, and Cu/SiO_2 catalyst exhibited the best catalytic performance. FAL conversion and selectivity of 2-MF were respectively as high as 100% and 89.5% under atmospheric pressure, 220 °C, WHSV=0.5h^{-1}. Systematic characterizations demonstrated that Cu/SiO_2 catalyst had some major advantages, such as (1) a higher copper dispersion, (2) a more adequate weak acid sites which emerged by the interaction of copper-silicon, and (3) a lower desorption temperature of desired product 2-MF than Cu/Al_2O_3 and Cu/ZnO catalysts. It is suggested that the intrinsic properties of support have significant influence on the catalytic performance of Cu-catalysts. Meanwhile, temperature also played an important role in determining selectivity of 2-MF. In gas-phase hydrogenation of FAL to 2-MF, the evolution of catalytic activity and products distribution over three supported Cu-catalysts suggested synergistic effect of copper dispersion and the acidic property, which activates the -CH=O group of reactant FAL and dissociates the -CH_2-OH group of the intermediate FOL. Based on our studies, SiO_2 support would be considered a promise candidate to prepare Cu-based catalysts with the high activity in the hydrogenation of FAL to bio-fuel 2-MF.

Acknowledgments

The authors gratefully thank the financial supports of Major State Basic Research Development Program of China (973 Program) (No. 2012CB215305).

References

[1] D.M. Alonso, S. G. Wettstein, J. A. Dumesic, Chem. Soc. Rev. 41 (2012) 8075-8098.
[2] P. Gallezot, Chem. Soc. Rev. 41 (2012) 1538-1558.
[3] J.A. Melero, J. Iglesias, A. Garcia, Energy Environ. Sci. 5 (2012) 7393-7420.
[4] I. Agirrezabal-Telleria, I. Gandarias, P.L. Arias, Bioresour. Technol. 143 (2013) 258-264.
[5] M. Grilc, B. Likozar, J. Levec, Appl. Catal. B: Environ. 150– 151 (2014) 275– 287.
[6] M. Grilc, B. Likozar, J. Levec, Biomass Bioenerg. 63 (2014) 300-312.
[7] B. Danon, G. Marcotullio, W. de Jong, Green. Chem. 16 (2014) 39-54.
[8] A.P. dunlop, Ind. Eng. Chem. 40 (1948) 204-209.
[9] V. Pace, P. Hoyos, L. Castoldi, P. Dominguez de Maria, A.R. Alcantara, ChemSusChem. 5 (2012) 1369-1379.
[10] N.S. Biradar, A.M. Hengne, S.N. Birajdar, P.S. Niphadkar, P.N. Joshi, C.V. Rode, ACS Sustainable Chem. Eng. 2 (2014) 272-281.
[11] M. Besson, and C. Pinel, Chem. Rev. 114 (2014) 1827-1870.
[12] C. Wang, H. Xu, R. Daniel, A. Ghafourian, J.M. Herreros, S. Shuai, X. Ma, Fuel 103 (2013) 200-211.
[13] X. Ma, H. Xu, H. Ding, S. Shuai, Fuel 116 (2014) 281-291.
[14] S. Sitthisa, D.E. Resasco, Catal. Lett. 141 (2011) 784-791.
[15] L.W. Burnette, I.B. Johns, R.F. Holdren, R.M. Hixon, Ind. Eng. Chem. 40 (1948) 502-505.
[16] K. Yan, A. Chen, Fuel 115 (2014) 101-108.
[17] J.Y. Lee, D.W. Lee, K.Y. Lee, Y. Wang, Catal. Today. 146 (2009) 260-264.
[18] B.M. Nagaraja, V. Siva Kumar, V. Shasikala, A.H. Padmasri, B. Sreedhar, B. David Raju, K.S. Rama Rao, Catal. Commun. 4 (2003) 287-293.
[19] R.S. Rao, R.T.K. Baker, M.A. Vannice, Catal. Lett. 60 (1999) 51-57
[20] S. Sitthisa, W. An, D. E. Resasco, J. Catal. 284 (2011) 90-101.
[21] Kai Yan, Aicheng Chen, Energy. 58 (2013) 357-363.
[22] R. Rao, A. Dandekar, R. T. K. Baker, M. A. Vannice, J. Catal. 171 (1997) 406-419.
[23] L.Chen, Y. Zhu, H. Zheng, C. Zhang, B. Zhang, Y. Li, Appl. Catal. A: Gen. 411-412 (2012) 95-104. □□□□
[24] A. Gutierrez, R.K. Kaila, M.L. Honkela, R. Slioor, A.O.I. Krause, Catal. Today. 147 (2009) 239-246.
[25] C. Zhao, Y. Kou, A. Lemonidou, X. Li, J.A. Lercher, Angew. Chem. Int. Ed. 48 (2009) 3987-3990.
[26] K. Murata, Y. Liu, M. Inaba, I. Takahara, Energy & Fuels 24 (2010) 2404-2409.
[27] H. Zheng, Y. Zhu, B. Teng, Z. Bai, C. Zhang, H. Xiang, Y. Li, J. Mol. Catal. A: Chem. 246

(2006) 18-23.
[28] Z. He, H. Lin, P. He, Y. Yuan, J. Catal. 277 (2011) 54–63.
[29] J. Gong, H. Yue, Y. Zhao, S. Zhao, L. Zhao, J. Lv, S. Wang, X. Ma, J. Am. Chem. Soc. 134 (2012) 13922-13925.
[30] K.L. Deutsch, B.H. Shanks, J. Catal. 285 (2012) 235-241.
[31] Guoqiang Ding, Yulei Zhu, Hongyan Zheng, Wei Zhang, Yongwang Li, Catal. Commun. 11 (2010) 1120–1124.
[32] A. Yin, X. Guo, W. Dai, K. Fan, J. Phys. Chem. C. 113 (2009) 11003-11013.
[33] Z. Huang, F. Cui, J. Xue, J. Zuo, J. Chen, C. Xia, Catal. Today. 183 (2012) 42-51.
[34] P. Burattin, M. Che, C. Louis, J. Phys. Chem. B. 102 (1998) 2722-2732.
[35] Z. Liu, M.D. Amiridis, Y. Chen, J. Phys. Chem. B. 109 (2005) 1251-1255.
[36] K.V.R. Chary, K.K. Seela, G.V. Sagar, B. Sreedhar, J. Phys. Chem. B. 108 (2004) 658-663.
[37] J.B. Wang, D.H. Tsai, T.J. Huang, J. Catal. 208 (2002) 370-380.
[38] U.R. Pillai, S. Deevi, Appl. Catal. B: Environ. 65 (2006) 110-117.
[39] D.G. Manly, A.P. Dunlop, J. Org. Chem. 23 (1958) 1093-1095.
[40] H. Atia, U. Armbrusterb, A. Martinb, J. Catal. 258 (2008) 71-82.
[41] P. Bera, S. Mitra, S. Sampath, M.S. Hegde, Chem. Commun. (2001) 927-928.
[42] T.H. Fleisch, G.J. Mains, Appl. Sur. Sci. 10 (1982) 51-62.
[43] G. Anger, A. Winkler, K.D. Rendulic, Sur. Sci. 220 (1989) 1-17.
[44] T. Genger, O. Hinrichsen, M. Muhler, Catal. Lett. 59 (1999) 137–141
[45] J.T. Miller, B.L. Meyers, F.S. Modica, G.S. Lane, M. Vaarkamp, D.C. Koningsberger, J. Catal. 143 (1993) 395-408.
[46] I. Melian-Cabrera, M. Lopez Granados, J.L.G. Fierro，J. Catal. 210 (2002) 285-294.
[47] J.G. Stevens, R.A. Bourne, M.V. Twigg, M. Poliakoff, Angew. Chem. 122 (2010) 9040-9043.
[48] M. Boudart, Chem. Rev. 95 (1995) 661-666.
[49] S. Sitthisa, T. Sooknoi, Y. Ma, P. B. Balbuena, D.E. Resasco, J. Catal. 277 (2011) 1-13.
[50] L. Chen, P. Guo, M. Qiao, S. Yan, H. Li, W. Shen, H. Xu, K. Fan, J. Catal. 257 (2008) 172-180.
[51] Y. Zhu, H. Xiang, G. Wu, L. Bai, Y. Li, Chem. Commun. (2002) 254-255.

Scheme1 The main reaction pathway of furfural hydrogenation over the Cu-catalysts.

FAL, furfural; FOL, furfuryl alcohol; 2-MF, 2-methylfuran; 2-MTHF, 2-methyltetrafuran; THFOL, tetrahydrofurfuryl alcohol; FU, furan; THF, tetrahydrofuran; 2-PO, 2-pentanone; 2-PL, 2-pentanol; 1-PL, 1-pentanol.

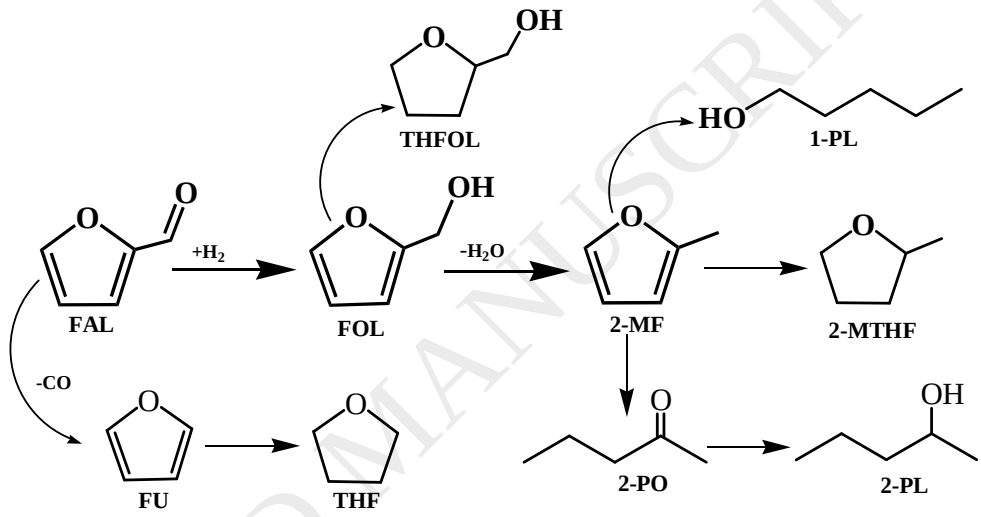

Figure Captions

Fig. 1 XRD patterns of the calcined catalysts at 450 ℃.

Fig. 2 H_2-TPR profiles of the calcined catalysts.

Fig. 3 (A) Cu 2p photoelectron spectra of the calcined catalysts, (B) Cu 2p photoelectron spectra of the reduced catalysts, (C) Cu LMM XAES spectra of the reduced catalysts.

Fig. 4 NH_3-TPD profiles: (A) the reduced catalysts; (B) Cu/Si catalysts.

Fig. 5 H_2-TPD profiles of the reduced catalysts.

Fig. 6 FAL-TPD experiments of the reduced catalysts: (A) FAL desorption, m/e=96; (B) FOL

desorption from the reaction of FAL, m/e=98; (C) 2-MF desorption from the reaction of FAL, m/e=82; (D) H_2O desorption from the reaction of FAL, m/e=18.

Fig. 7 The long term stability of Cu/SiO_2 catalyst, Reaction conditions: pure furfural, 220 °C, atmospheric pressure, H_2/furfural = 17:1 (molar ratio), WHSV = 0.5 h^{-1}.

Fig. 8 TEM images of the fresh and spent Cu/SiO_2 catalysts.

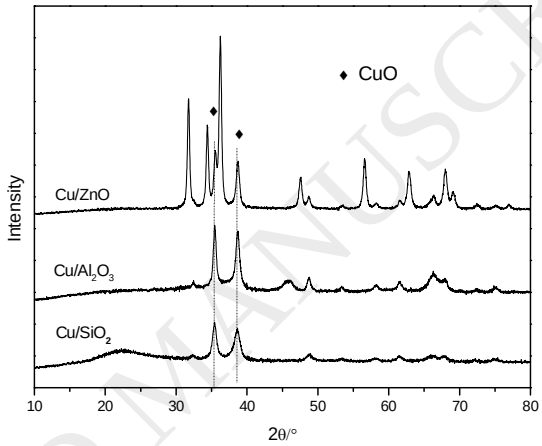

Fig. 1

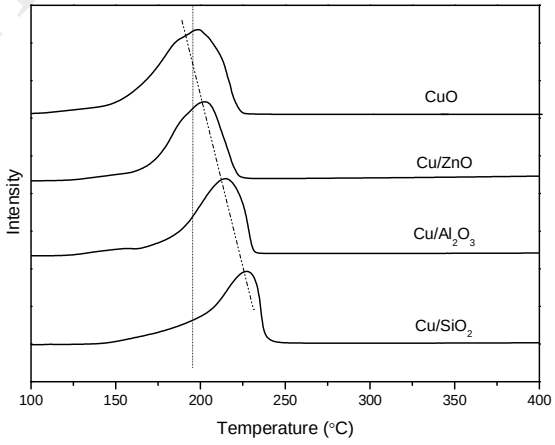

Fig. 2

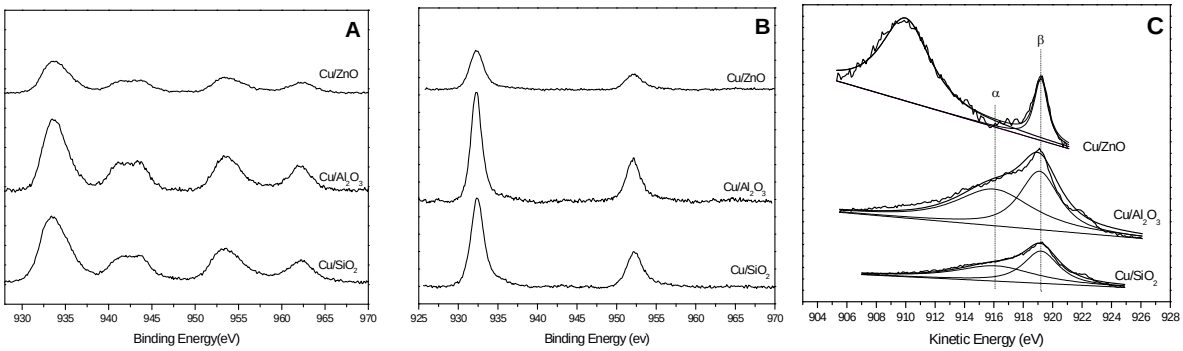

Fig. 3

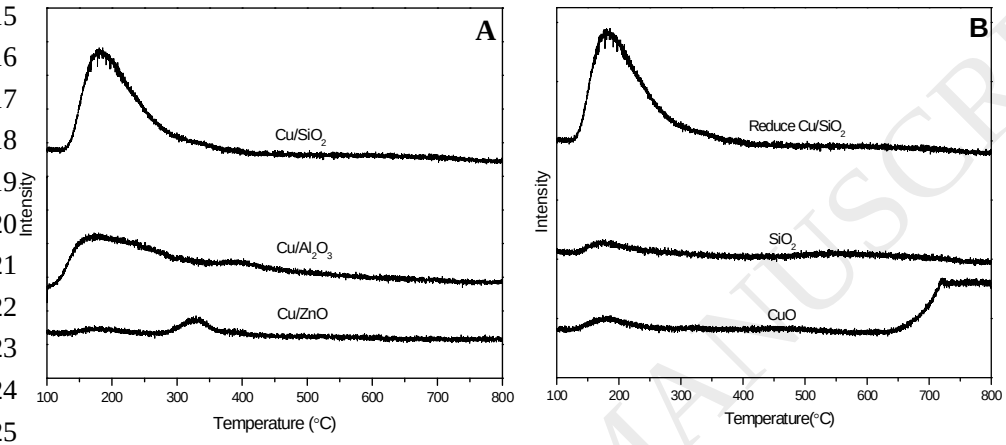

Fig 4

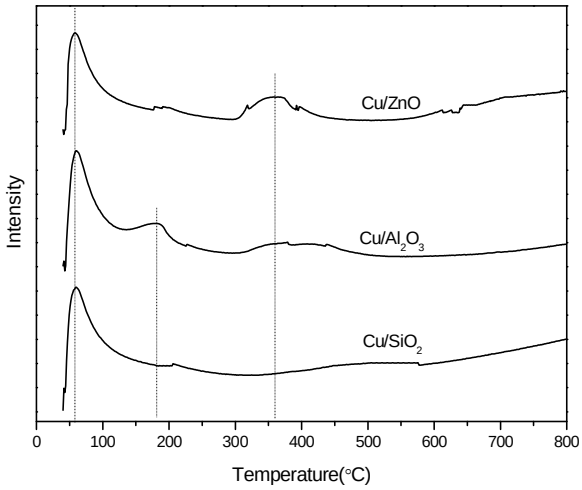

Fig. 5

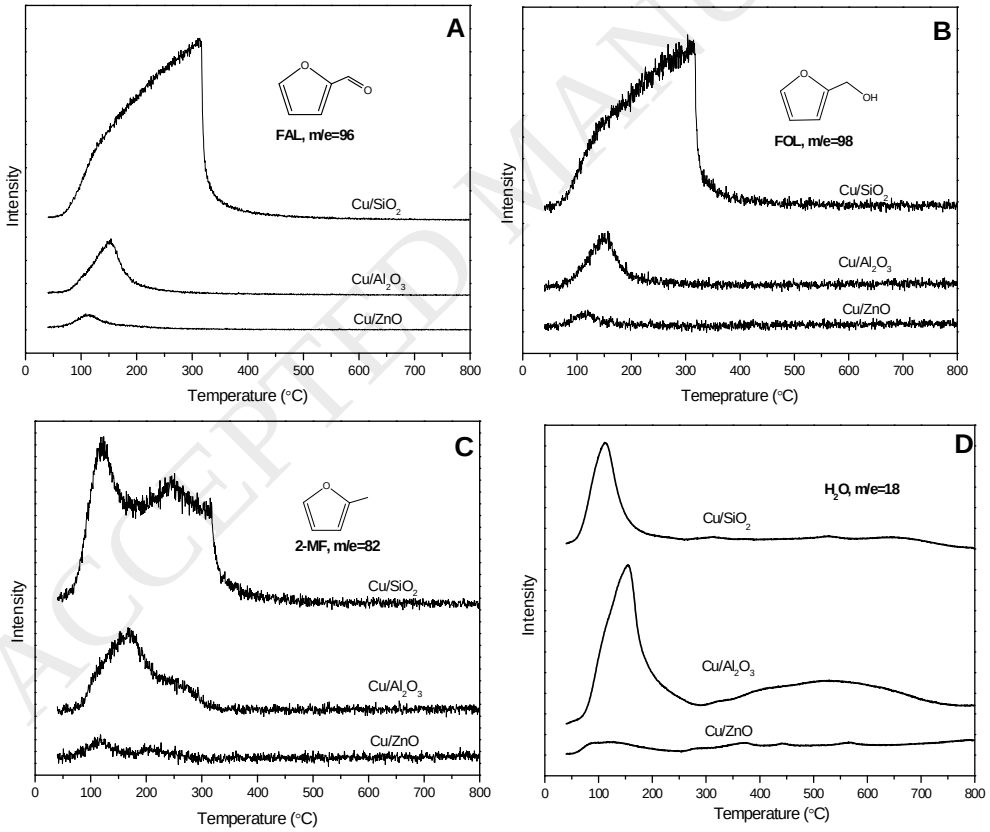

Fig. 6

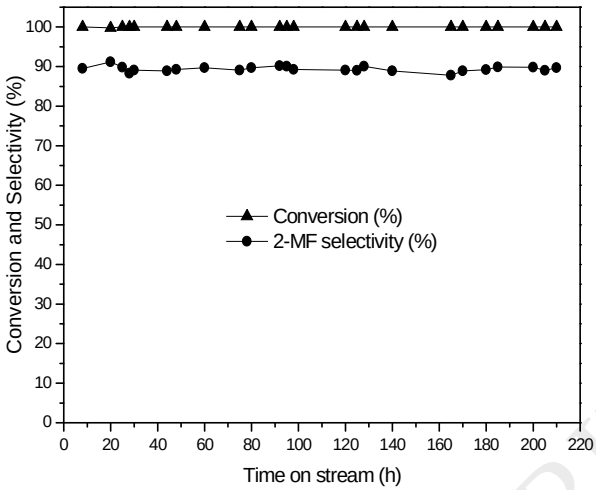

Fig. 7.

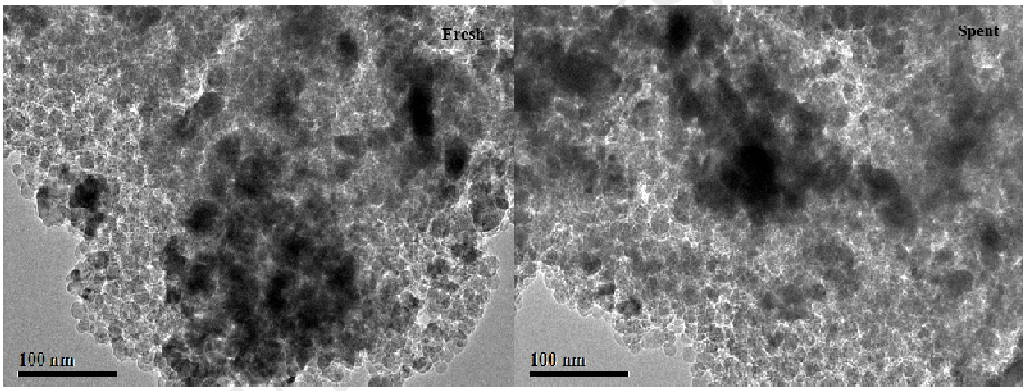

Fig. 8

Table 1 The physicochemical properties of the supported Cu-catalysts

Catalysts	S_{BET} ($m^2.g^{-1}$)[a]	D_{pore} (nm)[a]	V_{pore} ($cm^3.g^{-1}$)[a]	Cu content (%)[b]	d_{CuO} (nm)[c]	d_{Cu} (nm)[d]	D_{Cu} (%)[d]	S_{Cu} ($m^2.g^{-1}$)[d]	$X(Cu^+/Cu^0)$ (mol/mol)[e]
Cu/SiO_2	161.4	8.7	0.430	22.9	8.45	5.97	16.76	25.67	2.23
Cu/Al_2O_3	124.8	9.0	0.372	26.0	11.37	6.46	15.47	27.29	1.93
Cu/ZnO	14.9	29.4	0.134	23.5	14.51	12.31	8.13	12.93	0.91

[a] Determined by N_2-adsorption method

[b] Determined by ICP.

[c] Average Cu particle size calculated by Scherrer equation.

[d] Determined by N_2O chemisorption.

[e] Determined by XAES.

Table 2 Furfural conversion and selectivity of the products over the supported Cu-catalysts [a]

Catalysts	Conversion（%）	TOF(h^{-1})	Selectivity(%)[b]			
			2-MF	FOL	RO	Others
Cu/SiO_2	100	24.3	89.5	2.4	6.0	2.1
Cu/Al_2O_3	99.2	7.1	71.6	10.7	4.9	12.8
Cu/ZnO	94.5	5.8	65.3	32.9	0.4	1.4

[a] using pure furfural at 220°C , atmospheric pressure , WHSV=0.5h^{-1}, H_2/FAL=17

[b] 2-MF=2-methylfuran, FOL=furfuryl alcohol, RO=the ring open products(i.e. 2-pentanone, 1-pentanol, 2-pentanol), Others= furan, 2-methyltetrahydrofuran, tetrahydrofurfuryl alcohol, furfural polymers

Table 3 Hydrogenation of furfural to 2-methylfuran

Catalysts	Reaction conditions	Sel /% (Con /%)	Ref
$Ni\text{-}Fe/SiO_2$	250 °C, H_2/FAL=25, W/F=0.1 h	39.1(96.3)	[20]
Cu: Zn: Al: Ca: Na	250 °C, H_2/FAL=25, WHSV=0.3 h^{-1}	87(99.7)	[27]
Cu/Cr	240 °C, Supercritical CO_2,	90	[47]
Cu/SiO_2	220 °C ,H_2/FAL=17, WHSV=0.5 h^{-1}	89.5(100)	this work

Table 4 Influence of the reaction temperature and weight hourly space velocity for furfural hydrogenation over Cu/SiO_2 catalyst [a]

WHSV(h^{-1})	T(ºC)	Conversion (%)	Selectivity (%)[b]			
			2-MF	FOL	RO	Others
0.5	140	98.3	20.7	73.8	0.1	5.4
2.0	140	63.2	1.8	98.2	0	0
0.5	160	99.8	40.9	57.9	0.4	0.8
2.0	160	76.8	17.5	82.1	0.2	0.2

0.5	180	99.9	71.2	27.0	0.5	1.3
2.0	180	95.7	27.1	72.3	0.3	0.3
0.5	200	100	77.2	14.3	4.4	4.1
2.0	200	96.7	49.4	49.7	0.5	0.4
0.5	220	100	89.5	2.4	6.0	2.1
2.0	220	100	77.5	17.4	0.3	4.8

[a] using pure furfural at atmospheric pressure, H_2/FAL=17.

[b] 2-MF=2-methylfuran, FOL=furfuryl alcohol, RO=the ring open products(i.e. 2-pentanone, 1-pentanol, 2-pentanol), Others = furan, 2-methyltetrahydrofuran, tetrahydrofurfuryl alcohol, furfural polymers